

تأثير التلدين على الخصائص التركيبية والبصرية للغشاء الرقيق

المحضر بطريقة الترسيب بالليزر النبضي $\text{Pb}(\text{Zr}_{0.7}, \text{Ti}_{0.3})\text{O}_3$

عبد الكريم دهش علي غصون حميد محمد حميد عبد الله رضوان كاظم عبد الواحد

عادم

جامعة تكريت/كلية التربية/قسم الفيزياء جامعة بغداد/كلية العلوم/قسم الفيزياء جامعة تكريت/كلية التربية/قسم الفيزياء

الفيزياء

kadhim-adem@yahoo.com,

ham2348378@gmail.com

ghuson.Hamed@yahoo.com

Abdulkerem.Ali@tu.edu.iq

أخلاصة

حضر مسحوق $\text{Pb}(\text{Zr}_x, \text{Ti}_{1-x})\text{O}_3$ (PZT) بطريقة تفاعل الحالة الصلبة ورسب على الزجاج بالليزر النبضي. أظهرت دراسة الخصائص التركيبية للغشاء عند $x=0.7$ بواسطة حيود الاشعة السينية ان الغشاء متعدد التبلور مع وجود عدة قمم. وظهرت فحوصات مجهر القوة الذرية لدراسة طوبوغرافية السطح للعينات بان الحجم الحبيبي بحدود 100 nm يقل الى حوالي 70 nm بعد التلدين الى 723 K. درست الخصائص البصرية للغشاء ضمن نطاق الاطوال الموجية المرئية وتحت الحمراء عند درجة حرارة الغرفة وبعد التلدين عند 723 K وسجلت الامتصاصية والنفاذية لمدى طول موجي (390-1100) nm وكذلك درست الخصائص البصرية ووجد ان فجوة الطاقة البصرية (E_g) تزداد بعد التلدين وتكون بقية الخصائص كذلك حساسة للتغير بدرجة الحرارة. اجريت تحليلات فورير للاشعة تحت الحمراء لمعرفة هوية الغشاء ووجد انه يعاني من المط عند العدد الموجي (3477.66 cm^{-1}) بعد التلدين بدرجة حرارة 723 K. استخدم جهاز مقياس التداخل (جهاز مايكلسون) لقياس سمك الغشاء وكان بحدود 200 نانومتر.

الكلمات الدالة: تأثير التلدين، الترسيب بالليزر النبضي، خصائص غشاء $\text{Pb}(\text{Zr}_{0.7}, \text{Ti}_{0.3})\text{O}_3$.



Annealing temperature effect on the Structural and Optical properties of $\text{Pb}(\text{Zr}_{0.7}\text{Ti}_{0.3})\text{O}_3$ thin film prepared by Pulsed Laser Deposition (PLD)

Abdul Kareem Dahash Ali , Ghuson Hamed , Hameed Abdulla
Radwan , Kadhim A. Adem

University of Tikrit/College Of Education, University of Baghdad/College Of Science, University of Tikrit/College Of Education, University of Baghdad/College of Science

Abdulkerem.Ali@tu.ed.iq , ghuson.Hamed@yahoo.com ,
ham2348378@gmail.com , kadhim-adem@yahoo.com

Abstract:

$\text{Pb}(\text{Zr}_x\text{Ti}_{1-x})\text{O}_3$ (PZT) powder was prepared via solid-state reaction and deposited on glass by Pulsed Laser Deposition (PLD). X-ray diffraction (XRD) analysis carried out to investigate the phase structure, it was found that PZT thin films with $x=0.7$ are polycrystalline with many peaks, and the results of Atomic Force Microscopy (AFM) used to studied the samples topographic indicated the film have grain size around 100 nm decrease to around 70 nm after annealing to 723 K. The optiical properties of PZT films with $x=0.7$ studied at RT and 723 K. The absorbance and transmittance spectra have been registered in the wavelength range (390-1100) nm so as to examine the optical properties at vis-IR wavelengths. It was investigated that the optical energy gap (E_g) increase when annealing temperature (T_a) increase. An extinction coefficient, refractive index, real and imaginary dielectric constant were sensitive to the change in temperature. Fourier Transform Infra-Red (FTIR) to know the identity and to study the vibrational frequencies between the bonds of atoms for synthesized (PZT) Nanoparticles which found stretching at (3477.66 cm^{-1}) after





annealing to 723 K. the interferometer used to determine the thickness of the deposited film, it found of about 200 nm.

Keyword: Annealing effect, PLD, $\text{Pb}(\text{Zr}_{0.7}\text{Ti}_{0.3})\text{O}_3$ film Properties.

Introduction:

Due to the great interest and concentration of nano-crystal semiconductor technology has attracted applications. Magnetic, optical and electrical dependent on the particle size of the particles [1]. Perovskite $\text{Pb}(\text{Zr}, \text{Ti})\text{O}_3$ (PZT) family is one of the most popular materials for a wide range of applications, ferroelectric, piezoelectric and Pyroelectric [2,3], The technology of thin films is a valuable tool in the development of modern electronic devices has become. Recently, ferroelectric lead zirconium titanate, $\text{Pb}(\text{Zr}_x\text{Ti}_{1-x})\text{O}_3$ (PZT) thin films have been extensively used for applications in many high technology fields due to their excellent ferroelectric properties, such as: high dielectric constants, high remanent polarization and large piezoelectric coefficient, qualities of great importance in device applications as in, for instance, the construction of low-energy-consumption, high-speed and radiation-hard ferroelectric nonvolatile random-access memories (NVRAM), or the development of pyroelectric detectors [4, 5]. Preparation of epitaxial PZT films has been performed using several techniques such as radio frequency magnetron sputtering, metal organic chemical vapor deposition (MOCVD), pulsed laser ablationetc. [6]. Laser ablation Physical- itself as one of the most efficient method for building nanostructures with respect to its control, the costs are relatively modest, and



has shown flexibility [7,8] The method is to destroy a target by an intense laser beam returns to the exit of its components and the formation of nanoclusters and nanostructures [9] . PZT energy band gap is of about 3.4 eV. Valence band mainly composed of oxygen 2P states, while empty groups are guided by the states Ti^{4+} or Zr^{4+} d is formed. The main characteristic that distinguishes PZT perovskite titanates is the electronic structure of the Pb^{2+} ions. These retain their 6s electrons, the so-called inert pairs in the valence band. Using the tight-binding, Robertson and colleagues [10] calculated that the upper valence band states are actually composed of Oxygen 2P and lead 6S [11]. The aim of this work is to build and analyze the structural and optical characteristics of thin films of lead (Zr_x, Ti_{1-x}) O_3 processing method using pulse laser deposition (PLD).

Experimental procedure:

Bulk samples of $Pb(Zr_x, Ti_{1-x})O_3$ have been prepared by solid-state reaction process. The powder of Lead dioxide , Zirconium dioxide and Titanium dioxide with a purity of 99.99% were Grinded and mixed together at a concentration $x = 0.7$ of the formula $Pb(Zr_x, Ti_{1-x})O_3$ in a mixture machine for 10 minutes. After that it was pressed into pellets with 1.2 cm diameter and 0.2 cm thick, using hydraulic piston type (SPECAC), under the pressure of 6 tons/cm² for 10 minutes. The pellets were sintered in a controller furnace to temperature 1073 K for two hours then cooled to room temperature. The substrate used in this work for deposit of $Pb(Zr_{0.7}, Ti_{0.3})O_3$ thin films is the glass slides made in china from " AFco", with dimensions (75 × 25 × 1.2) mm. The substrate cleaned in the following steps:

1-The substrates were cleaned in distilled water to remove the impurities and residual grime from their surface.

2-The substrates were cleaned in alcohol by an ultrasonic system for 15 min in order to remove grease and some oxides, and dried by blowing air.

3-Eventually, the slides were wiped with soft paper.

The structure of $Pb(Zr_x, Ti_{1-x})O_3$ films studied by X-ray diffraction using a Philips X-ray diffraction system that records the intensity as a function of Bragg's angle is investigated. The wavelength of the radiation source $Cu K\alpha = 1.5405 \text{ \AA}$, 20 mA current and the voltage was 30 kV. 2θ scan angle in the range (20-70) degree at 2cm.min-1 speed. interplane distance d (hkl) to various pages was determined using Bragg's law[12]:

$$n\lambda = 2d \sin\theta \dots\dots\dots(1)$$

Where n is the order of reflection.

Fixed lattice of relations estimate:

$$d = a / (h^2 + k^2 + l^2)^{1/2} \dots\dots\dots(2)$$

$Pb(Zr_x, Ti_{1-x})O_3$ grain size (D) can be calculated by using the Scherrer equation [13]:

$$D = K^* \lambda / \beta \cos\theta \dots\dots\dots(3)$$

Where: θ is the diffraction angle, β full width half maximum.

Studies using atomic force microscopy (Scanning probe microscope type AA3000), supplied by the Angstrom Advanced Company to determine the grain size and roughness for Lead $Pb(Zr_x, Ti_{1-x})O_3$ glass base was recorded and their statistical distribution . The atomic force microscope (AFM) topographic mapping has three main modes: contact, contactless we morphology were used in research and intermittent contact or tapping.

Optical properties of films with different content of x in $Pb(Zr_x, Ti_{1-x})O_3$ deposited on the substrate and different annealing temperature at a wavelength of about (190-390) nm and (390-1100) nm using UV / VIS Centra 5 spectrometer

that previous GBC Scientific Equipment PTY LTD. The spectrometer consists of two deuteriums and tungsten lamp light source at a wavelength of 190-390 nm and 390-1100 nm range of the spectrum. Data output wavelength, transmission and absorption in a computer program used to deduce the optical energy gap and the underlying edge optical and optical constant.

Fixed optical parameters are very important because they describe the optical behavior of materials. Energy absorption coefficient of a material is a function of photon energy band gap is very strong. Indicates a weakening of the incident photon energy absorption coefficient per unit thickness passing through a material. The main reason for this attenuation processes of absorption attributed [14,15]. Optical constants of refractive index (n_c), extinction coefficient (k), and real (ϵ_r), and imaginary components (ϵ_i) of the dielectric constant. The complex refractive index (n_c) is defined as [16]:

$$n_c = n - ik \dots \dots \dots (4)$$

It is related to the velocity of propagation (v) and light velocity (c) By:

$$v = \frac{c}{n_c} \dots \dots \dots (5)$$

refractive index can be calculated from the formula [12]:

$$n = \left(\frac{4R}{(R-1)^2} - k^2 \right)^{1/2} - \frac{(R+1)}{(R-1)} \dots \dots \dots (5)$$

where R is the reflectance and can be expressed by the relation [15]:

$$R = \frac{(n-1)^2 + k^2}{(n+1)^2 + k^2} \dots \dots \dots (7)$$

Extinction coefficient that corresponds to the exponential decay of the wave as it passes through the material, as defined [14]:

$$k = \frac{\alpha\lambda}{4\pi} \dots \dots \dots (8)$$

(α) is given by :

$$\alpha = 2.303 \frac{A}{t} \dots \dots \dots (9)$$

Where A is absorbed. The real and imaginary parts of the optical dielectric constant can be calculated using the following equation [16]:

$$(n - ik)^2 = \varepsilon_r - \varepsilon_i \dots \dots \dots (10)$$

where

$$\varepsilon_r = n^2 - k^2 \dots \dots \dots (11)$$

and

$$\varepsilon_i = 2nk \dots \dots \dots (12)$$

the basis scan FTIR In the range between (400-4000) cm⁻¹ was carried out. The purpose of this analysis is to provide more details on production Phase powder and identity.

Result and Discussion:

X- ray diffraction testing on Pb(Zr_{0.7}Ti_{0.3})O₃ thin film at room temperature showed a polycrystalline rhombohedral structure [17][11]. the reflections were (111), (110) and (202) which corresponding to $2\theta = 30.2703^\circ, 30.8784^\circ$ and 50.4054° respectively. After annealed to 723 K it can be notice that the peaks were (012), (130), (400), (101), (111), (200), (112) and (121) corresponding to $2\theta = 21.6327^\circ, 22.5850^\circ, 29.1156^\circ, 31.6100^\circ, 39.2290^\circ, 46.1678^\circ$ and 55.6463° respectively. A polycrystalline structure with impurity phase is formed identified pyrochlore. The presence of (400) reflection means pyrochlore phase['8], which appear after annealing more than 423 K. A wide peaks indicate to coexistence of small crystal particles[19]. Using Scherrer's formula to find grain size as shown in table (1). We observed that the grain size decreases after

annealing samples to 723 K that is attributed to melting apart of Lead which have a low melting point and prominence a grains of Titanium and Zirconium on the surface. Generally, the mean grain size were decreased after the annealing procedure as shown in table (1) and fig.(1).

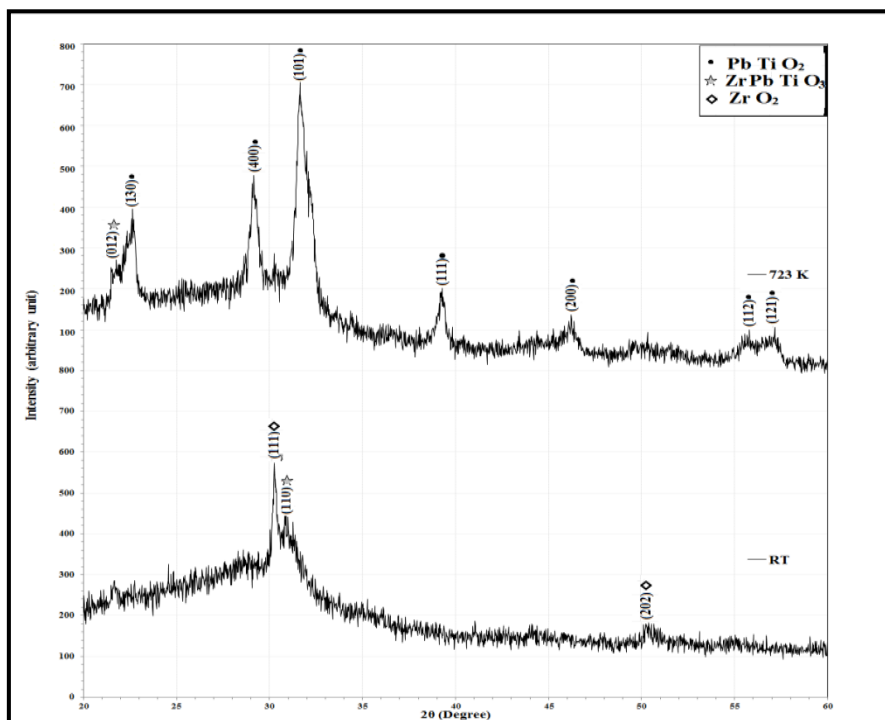


Fig.(1):X-rd of $\text{Pb}(\text{Zr}_{0.7}\text{Ti}_{0.3})\text{O}_3$ thin film at room temperature and 723K .

Table (1): Shows the peaks and its Bragg's angle, interplanar distance, and full width half at maximum for $\text{Pb}(\text{Zr}_{0.7},\text{Ti}_{0.3})\text{O}_3$ thin films at room temperatur and 723K.

T (K)	2θ (Deg.)	FWHM (Deg.)	d_{hkl} Exp.(Å)	G.S (nm)	d_{hkl} Std.(Å)	hkl	card No.
RT	30.2703	0.3379	2.9502	24.4	2.9613	(111)	96-500-0039
	30.8784	0.4729	2.8935	17.4	2.8890	(110)	96-210-2946
	50.4054	0.8108	1.8090	10.8	1.8134	(202)	96-500-0039
723	21.6327	0.4989	4.1047	16.2	4.0967	(012)	96-210-2946
	22.5850	0.6803	3.9338	11.9	3.9166	(130)	96-400-0724
	29.1156	0.6350	3.0646	12.9	3.0963	(400)	96-400-0725
	31.6100	0.7256	2.8282	11.4	2.8459	(101)	96-901-1193
	39.2290	0.4535	2.2947	18.6	2.2999	(111)	96-901-1193
	46.1678	0.7257	1.9647	11.9	1.9525	(200)	96-901-1193
	55.6463	0.7257	1.6504	12.4	1.6604	(112)	96-901-1193
	57.0522	0.8617	1.6130	10.5	1.6100	(121)	96-901-1193

Figures (2,3) show 2D and 3D- images for surface morphology of the $\text{Pb}(\text{Zr}_{0.7},\text{Ti}_{0.3})\text{O}_3$ thin films analyzed by (AFM) at RT and at annealing temperatures of 723 K. These images reveal that the average grain size are in nano scale and the films have improving structure with a high homogeneity without voids , This means that the films are highly dense structure and homogenous. Average grain size , surface roughness and root mean square are recorded in table (2) which illustrates that all these parameters decrease with annealing the films to temperature 723 K, These results are perhaps return to melting apart of Lead which have a low melting point as well as larger volume and prominence a smaller grains of Titanium and Zirconium on the surface.

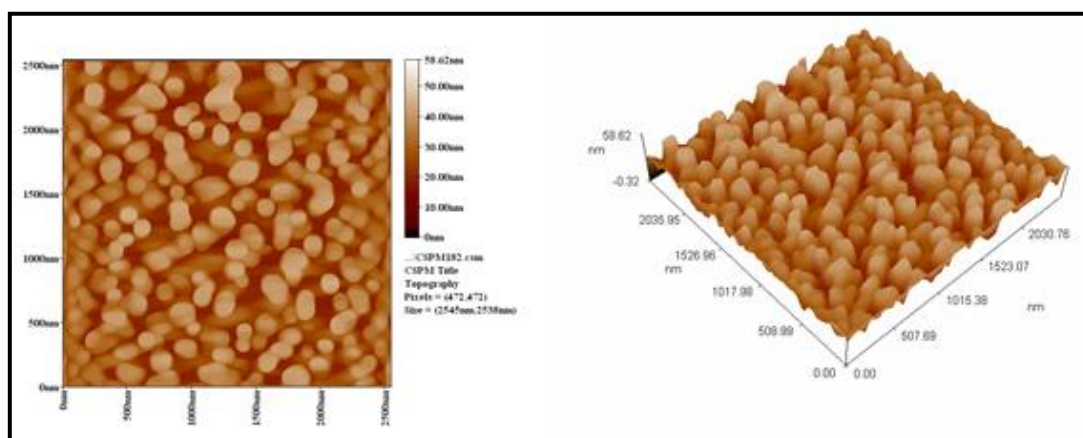


Figure (2): 2D and 3D images for surface morphology of the $\text{Pb}(\text{Zr}_{0.7}\text{Ti}_{0.3})\text{O}_3$ thin film analyzed by (AFM) at room temperature.

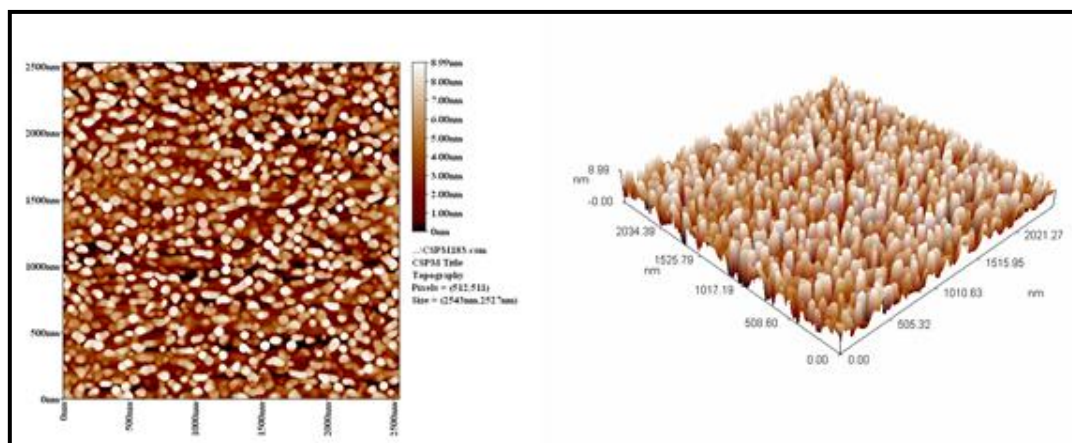


Fig. (3): 2D and 3D images for surface morphology of the $\text{Pb}(\text{Zr}_{0.7}\text{Ti}_{0.3})\text{O}_3$ thin film analyzed by (AFM) at annealing temperatures 723 K.

Table (٧): Average roughness, grain size and root mean square for the $\text{Pb}(\text{Zr}_{0.7}, \text{Ti}_{0.3})\text{O}_3$ thin films at room temperature and at annealing temperature 723 K obtained from (AFM).

$\text{Pb}(\text{Zr}_x, \text{Ti}_{1-x})\text{O}_3$	T (K)	Ave. Grain Size(nm)	RMS(nm)	Roughness(nm)
x = 0.7	RT	100.29	7.27	6.16
	723	68.78	2.58	2.24

The transmittance spectrum as a function of wavelength in the range of (390-1100)nm of $\text{Pb}(\text{Zr}_{0.7}, \text{Ti}_{0.3})\text{O}_3$ thin films deposited at room temperature and 723 K , it was noticed that the transmittance increases and shift to shorter wavelength with increasing of annealing temperature to 723 K as shown in figures (4) which is in agreement with Puustinen.[20] and Zak [21]. On the other hand, it is found that the value of the absorption coefficient (α) decreases with increasing of annealing temperature which is due to the increasing of energy gap as shown in table (3) and figure (5). The behavior of extinction coefficient (k) is approximately similar to the corresponding absorption coefficient. It can be observe from these figures that the extinction coefficient increases with the increasing of annealing temperature (T_a). The refractive index (n) decreases with increasing of the annealing temperature. This behavior may be happen due to the increment in energy gap which causes expansion of the bond length in the lattice and decreases the defect which means decreasing of the reflection where the refractive index depends on it which in agreement with Moret [22]. The real

(ϵ_r) and imaginary (ϵ_i) parts of dielectric constants were calculated by using the equations (11) and (12) respectively. (ϵ_r) behavior is similar to the refractive index of less value because of k^2 proportional to n^2 , while (ϵ_i) is mainly dependent on the value of k . The dielectric constants (ϵ_r) and (ϵ_i) are reversely proportional with the annealing temperature. The dielectric constants decrease with increasing of annealing temperature which is in agreement with [21] shown in table (3). Using Tauc equation to determine the values of the optical energy band gap (E_g) for $\text{Pb}(\text{Zr}_{0.7}\text{Ti}_{0.3})\text{O}_3$ films by plotting the relations $(\alpha h\nu)^r$ versus photon energy ($h\nu$) and select the optimum linear part. It was found that the relation for $r=2$ yields linear dependence, which indicates to the allowed direct transition. The optical energy band gap (E_g) of the films was calculated from the linear part of the plots of $(\alpha h\nu)^2$ versus photon energy ($h\nu$) to $\alpha=0$ as shown in figure (10). The values of the optical energy gap are increasing with the annealing temperature (T_a).

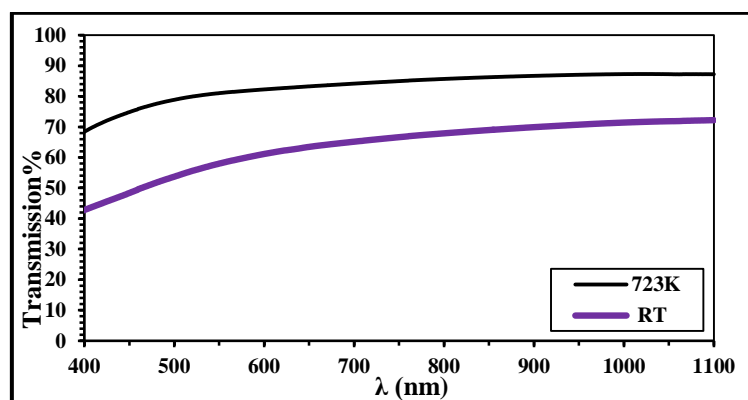


Figure (4): Transmittance spectrum as a function of wavelength for $\text{Pb}(\text{Zr}_{0.7}\text{Ti}_{0.3})\text{O}_3$ films at RT and 723 K .

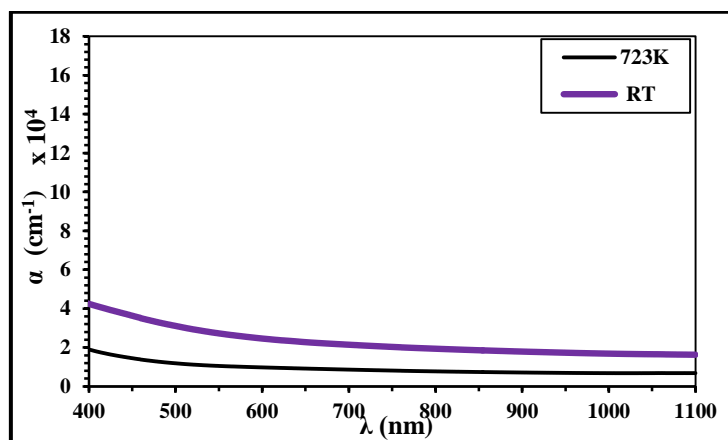


Figure (5): Absorption coefficient as a function of wavelength for $\text{Pb}(\text{Zr}_{0.7}\text{Ti}_{0.3})\text{O}_3$ films at RT and 723 K.

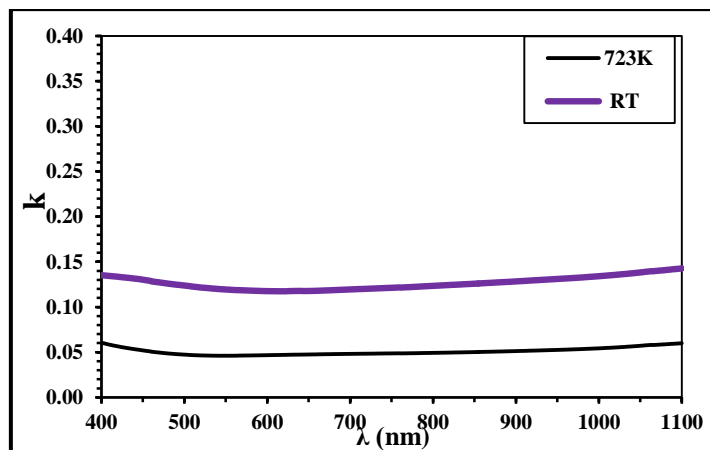


Figure (6): Extinction coefficient as a function of wavelength for $\text{Pb}(\text{Zr}_{0.7}\text{Ti}_{0.3})\text{O}_3$ films at RT and 723 K.

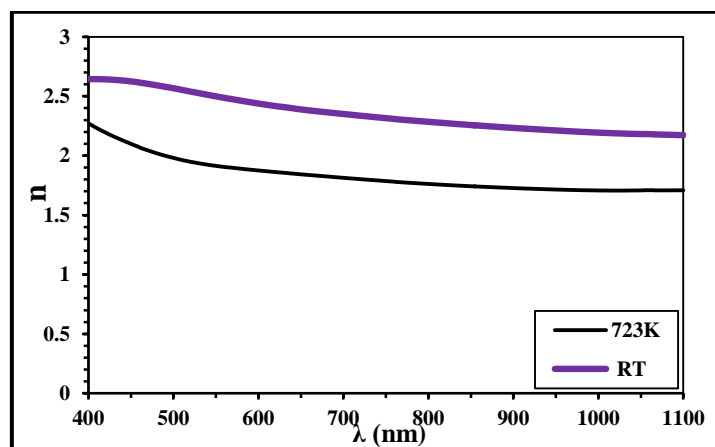


Figure (4): Refractive index as a function of wavelength for $\text{Pb}(\text{Zr}_{0.7},\text{Ti}_{0.3})\text{O}_3$ films at RT and 723 K.

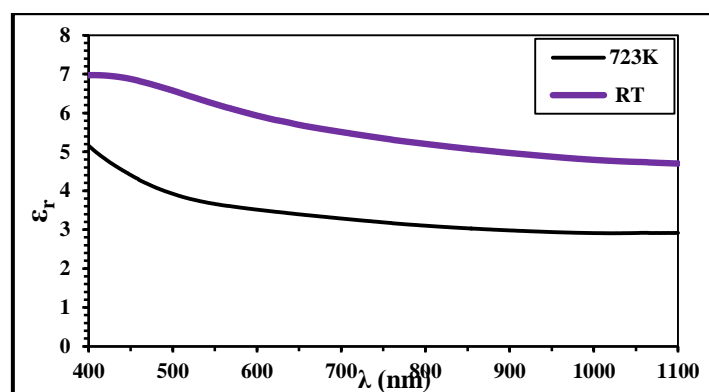


Figure (5): The variation of ϵ_r with wavelength for $\text{Pb}(\text{Zr}_{0.7},\text{Ti}_{0.3})\text{O}_3$ films at RT and 723 K.

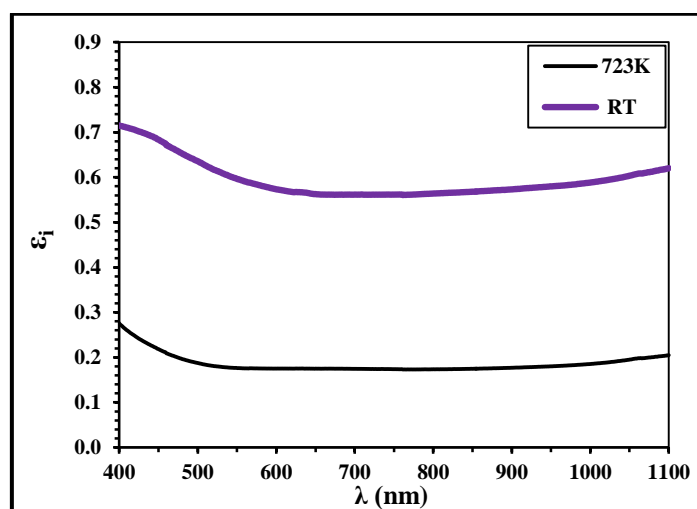


Figure (A): The variation of ϵ_i with wavelength for $\text{Pb}(\text{Zr}_{0.7},\text{Ti}_{0.3})\text{O}_3$ films at RT and 723 K.

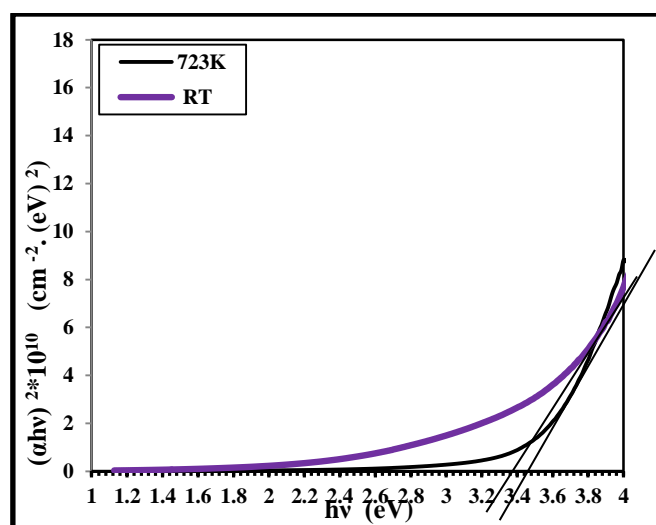


Figure (B): $(\alpha h\nu)^2$ as a function of $h\nu$ for $\text{Pb}(\text{Zr}_{0.7},\text{Ti}_{0.3})\text{O}_3$ films at RT and 723 K.

Table (C): Illustrates the transmission, absorption coefficient, extinction coefficient, refractive index, optical constants and energy band gap of $\text{Pb}(\text{Zr}_{0.7},\text{Ti}_{0.3})\text{O}_3$ films at RT and 723 K.

Ta (K)	x	T(%)	α (cm ⁻¹)	K	n	ϵ_r	ϵ_i	E _g (eV)
RT	0.7	53.8	31012	0.12	2.56	6.56	0.6	3.38
723	0.7	78.8	11918	0.05	2	3.9	0.19	3.47

Fig.(11) shows the absorption peaks noticed at (675.09 cm⁻¹) , (2361.23 cm⁻¹) and (3477.66 cm⁻¹) for sample at room temperature which can be indicated to the Pb(Zr_xTi_{1-x})O₃ vibrations. The absorption peak were decrease after annealing to 723 K due to increasing in transparency of the film which is in agreement with the optical measurements in this search. The presence of relatively broad band between 400 Cm⁻¹ to 800 Cm⁻¹ should be related to the establish of the Ti-O-Ti , Ti-O , Zr-O-Zr and Zr-O bonds, attached to C or Peroxyl groups also is an evidence for enhancement of perovskite

structure of PZT compound [23]. The absorption peak (2361.23 cm⁻¹) which corresponding to (C-H) bond were it is very sharp assigning to mono polar case. There a wake stretching in (3477.66 cm⁻¹) and a small shifting in peaks due to defect in structure resulting from growing in thickness. After annealed it can be observed from figure (12) that the (3477.66 cm⁻¹) were suffered from a high stretching with the annealing temperature this agree with Benam [24].

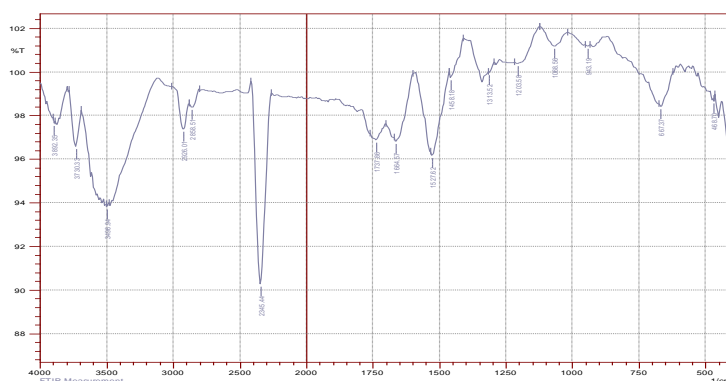


Figure (11):FTIR spectrum for $\text{Pb}(\text{Zr}_x\text{Ti}_{1-x})\text{O}_3$ thin films with $x=0.7$ at room temperature.

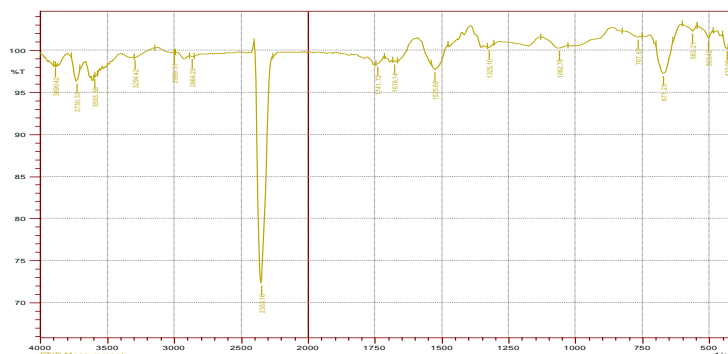


Figure (12):FTIR spectrum for $\text{Pb}(\text{Zr}_x\text{Ti}_{1-x})\text{O}_3$ thin films with $x=0.7$ at 723 K.

Conclusion:

X-ray diffraction results shows that the structure of PZT films is polycrystalline with rhombohedral structure. After annealed to 723 K an impurity phase is formed identified pyrochlore. AFM images show that the deposited $\text{Pb}(\text{Zr}_{0.7}\text{Ti}_{0.3})\text{O}_3$ layer on glass has a good situation, Average grain size , surface roughness and root mean square are decrease with annealing the film to temperature 723 K. The optical constants (absorption coefficient, refractive index, extinction coefficient, real and imaginary dielectric constant) of PZT are decrease, but the transmission and the energy band gap were decrease with the increasing of T_a . The film suffered from high stretch after annealed to 723 K. Fourier transform infra-red illustrate a wake stretching in (3477.66 cm^{-1}) and a small shifting in peaks due to defect in structure resulting from growing in thickness. After annealed the stretch (3477.66 cm^{-1}) were increased.



Kirkuk University Journal /Scientific Studies (KUJSS)

Volume 12, Issue 2, March 2017

ISSN 1992 – 0849

References:

- [1] R. Bargougui , K. Omri , A. Mhemdi and S. Ammar, "Synthesis and characterization of SnO₂ nanoparticles: Effect of hydrolysis rate on the optical Properties", Adv. Mater. Lett., Vol. 6, pp. 816-819, (2015).
- [2] W.C. Goh, K. Yao, C.K. Ong, Appl. Phys. A Mater. Sci. Process. 81, 1089, (2005).



Kirkuk University Journal /Scientific Studies (KUJSS)

Volume 12, Issue 2, March 2017

ISSN 1992 – 0849



- [3] C.T.Q. Nguyen, M.D. Nguyena, , , M. Dekkers , E. Houwmanb, H.N. Vua, G. Rijnders," Process dependence of the piezoelectric response of membrane actuators based on $\text{Pb}(\text{Zr}_{0.45}\text{Ti}_{0.55})\text{O}_3$ thin films," *Thin Solid Films* 556, 509–514, (2014).
- [4] J. Realpe, A. Cortes, E. Delgado, W. Lopera, & P. Prieto," Analysis of Hysteresis Measurements in Epitaxial SRO/PZT/Pt Capacitor Structures," *Ferroelectrics*, 335:233–240, (2006).
- [5] J. F. Scott and C. A. P. de Araujo,"Ferroelectric memories," *Science* 246, 1400–1405 (1989).
- [6] T. Matsunaga, T. Kamada, and R. Takayama," Crystallographic characterization of epitaxial $\text{Pb}(\text{Zr,Ti})\text{O}_3$ films with different Zr / Ti ratio grown by radio-frequency-magnetron sputtering," *Journal of applied Physics*, Vol. 93, No. 7, (2003).
- [7] P.R. Willmott, R. Timm, P. Felder, and J. R. Huber, *J. Appl. Phys.*,76, 2657, (1994).
- [8] K. A. Aadim, A. K. Hussain, M. R. Abdulameer," Effect of annealing temperature and laser pulse energy on the optical properties of CuO films prepared by pulsed laser deposition," *Iraqi Journal of Physics*, Vol.12, No.23, PP. 97-104, (2014).
- [9] W. M. Khilkhal, G. A. Al-Dahash & S. N. Abdul Wahid," Study the Effect of the Aqueous Media on the Properties of Produced Copper Nanoparticles Colloidal by Using Laser Ablation Technique,"*Eng. & Tech. Jornal*,Vol.33, part(B), No.4,(2014).
- [10] N.B. Chaim, M. Brunstein, J. Grunberg and A. Seidman, "Electric field dependence of the dielectric constant of PZT ferroelectric ceramics," *J. Appl. Phys.* 45, pp. 2398, (1974).
- [11] M. Pham," Ferroelectric Composites of PZT-Pt," Dissertation, University of Twente,(2005).
- [12] C. Kittel," Introduction to Solid State Physics," Eight Edit. John Wiley and Sons.,(2005).
- [13] L.V.Azaroff," Elements of X- ray Cryctallography," McGraw-Hill, Inc., (1968).
- [14] G. Burns, "Solid State Physics," New York: Academic Press, Inc, (1985).
- [15] J.Millman, "Microelectronics," Book Company Kogakusha: Murray – Hill, (1979).
- [16] S. Elliott, "Physics of Amorphous Materials," 1st edition. New York: Longman Inc, (1984).
- [17] B. Jaffe, W. Cook & H. Jaffe *Piezoelectric Ceramics*. Academic Press: 49–51, 135–171, (1971).





- [18] C. L. Elton & B. A. Eudes, "Phase transformations in PZT thin films prepared by polymeric chemical method," *Advances in Materials Physics and Chemistry*, (2012).
- [19] M. Prabu," Studies of pure and doped Lead Zirconate Titanate ceramics and PLD PZT thin films". PH.D Thesis, B.S. Abdur Rahman University ,(2013).
- [20] J. Puustinen, "Phase structure and surface morphology effects on the optical properties of nanocrystalline PZT thin films," *University of Oulu*, (2014).
- [21] A. K. Zak & W.H. Abd. Majid "Effect of solvent on structure and optical properties of PZT nanoparticles prepared by sol–gel method, in infrared region," *Ceram. Int.*, vol. 37, pp. 753–758, (2011).
- [22] M. Moret, M. Devillers & K. Worhoff, "Optical properties of PbTiO_3 , $\text{PbZr}_x\text{Ti}_{1-x}\text{O}_3$, and PbZrO_3 films deposited by metalorganic chemical vapor on SrTiO_3 ," *J. Appl. Phys.*, vol. 92, no. 1, pp. 468–474, (2002).
- [23] M. H. M. Zai, A. Akiba, H. Goto, M. Matsumoto, & E. M. Yeatman, "Highly \bar{Z} 111 . oriented lead zirconate titanate thin films deposited using a non-polymeric route," *Thin Solid Films*, pp. 97–101, (2001).
- [24] M. R. Benam," Monitoring the processing steps of Nano powders by FTIR technique", *IJRRAS*, 18, (2), (2014).





Kirkuk University Journal /Scientific Studies (KUJSS)

Volume 12, Issue 2, March 2017

ISSN 1992 – 0849



Kirkuk University Journal /Scientific Studies (KUJSS)

Volume 12, Issue 2, March 2017

ISSN 1992 – 0849